Hamid MEHADDENE[1], Hassane MOHELLEBI[1], Azouaou BERKACHE[1]

Department of Electrotechnics, Mouloud Mammeri University of Tizi Ouzou, Algeria (1)

doi:10.15199/48.2019.02.26

Eddy Currents Non Destructive Testing and Evaluation of Ferromagnetic Medium

***Abstract**. This work involves monitoring and non-destructive evaluation by inspecting two separate pieces (conductor and ferromagnetic). A database is established from the resolution of the direct problem. The inverse problem for the reconstitution of supposed single and multiple defects in the plates is then solved and analyzed. The study of the direct problem was made by exploiting the finite element method in resolution of the 2D magnetodynamic electromagnetic equation. Experimental Results are then performed and compared to simulation ones. The neural network technique was used successfully for the reconstruction of a single and multiple defects.*

Streszczenie.** W pracy zaprezentowano monitorowanie i nieniszczące badanie dwóch elementów – przewodzącego i ferromagnetycznego. Rozwiązanie problemu odwrotnego wykorzystano do rekonstrukcji defektu. Wykorzystano też metodę elementów skończonych do rozwiązania równań elektromagnetycznych 2D. Wykorzystano też sieć neuronową do rekonstrukcji kształtu pojedynczego i wielokrotnego defektu. **Nieniszczące badania ferromagnetycznego elementu metodą prądów wirowych

Keywords: Non destructive testing technique, Ferromagnetic materials, Eddy current, Finite element method, Artificial neural network.
Słowa kluczowe: badania nieniszczące, metoda prądów wirowych, metoda elementów skończonych,. Sieć neuronowa.

Introduction

There is nowadays an increasing attention and request towards the study and development of systems and techniques for increasing the human safety and security in all aspects of the everyday life. In this framework, the possibility to perform a non-invasive inspection of structures or objects by means of non-destructive testing and evaluation (NDT-NDE) technologies is of particular interests in several applicative fields, ranging from civil engineering to biomedicine, up to aeronautic and nuclear industries [1].

In non-destructive test methods, eddy current technology increasingly gains in importance. The reason for this is that it is a test method that is flexible in its application and that its probes, usually coils of copper wire, are very adaptable and can be produced fairly easily [2]. Eddy current non-destructive evaluation (NDE) is a method based on the fact that when a coil powered by a variable energy source is brought near a conductive part, a change in impedance at the terminals of the coil is driven by the changing of magnetic field lines due to the existence and the distribution of induced currents in the conductive part [3].

Besides the inspection of metallic samples for which ECT has been applied for some decades to detect cracks, voids, corrosion and other defect typologies structures [4, 5], this technique can also be used to distinguish between ferromagnetic and non-ferromagnetic materials.

However, this technique does not allow access to accurate information that can characterize a defect in any form; this is why it is essential to dispose for a rapid tool for signal inversion as eddy current. For this, we are interested in an artificial neural networks. This technique is capable of solving complex problems using an artificial reasoning system constructed with basis on the human brain [6]. A calculation tool developed under Matlab environment was used.

Simulation of direct problem with FEM

The relevant configurations is shown schematically in Fig. 1, consisting of a rectangular air core coil, an electrically conductive plate without a crack (a, b) and with a crack oriented along the x coordinate (c, d).

The work has two aspects; the first deals with the resolution of the direct problem, which solves the direct problem regardless of the complexity of the geometry of the studied system. The second deals with solving the inverse problem by exploiting neural networks while using databases from the direct digital model to achieve the desired parameters of the target.

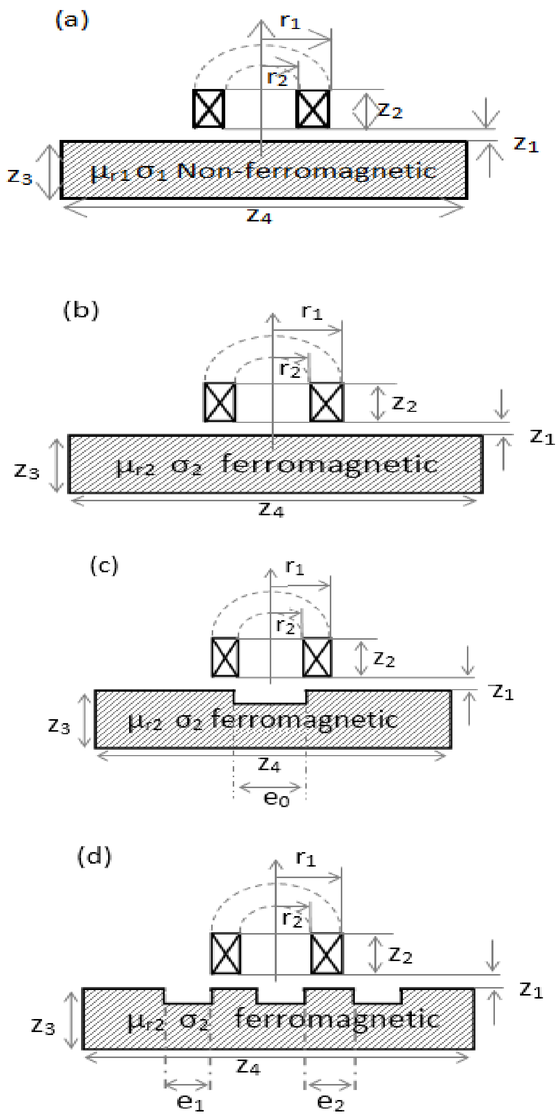

Fig.1. Studied electromagnetic configurations.

The first aspect has two approaches:

The first deals with the comparison of two types of healthy plate (a non-ferromagnetic μ_r = 1 and the other ferromagnetic $\mu_r \neq 1$) – Fig. 1(a) and 1(b).

The second deals with the detection of defects (single or multiple) in a ferromagnetic plate – Fig. 1(c) and 1(d).

Table 1. Physical and geometrical parameters

Sensor	Plate	Default
Outer radius r1= 9 mm	Length 80 mm	(c) Length e_0=6 mm Depth 0.5 mm
Inner radius r2= 2 mm	Thickness 1.25 mm	(d) Length e_1=2 mm Depth 0.5 mm
Width 1.5 mm	Conductivity: Non-ferromagnetic 37.7 M S/m ferromagnetic 1 Ms/m	-
Number of turns 120	Relative permeability 1.2	-
Frequency 1.4 - 1.6 kHz	Lift-off 0.2 mm	-
Current injected 1mA	-	-

Governing equations

The structures configurations with and without a crack are considered as shown in Fig. 1, where the source represents the exciting current in the coil, and the plate is the sample to be tested.

The eddy current problem can be described mathematically by the following partial differential equation in terms of the magnetic vector potential [7, 8]:

(1) $$-\frac{\partial}{\partial x}\left(\frac{1}{\mu}\frac{\partial A_z}{\partial x}\right)-\frac{\partial}{\partial y}\left(\frac{1}{\mu}\frac{\partial A_z}{\partial y}\right)+j\sigma\omega A_z = J_{sz}$$

$\vec{A} = (0,0,A_z)$, $\vec{J} = (0,0,J_z)$

where: σ – the electrical conductivity $[\Omega.m]^{-1}$, μ – the magnetic permeability $[H.m^{-1}]$, $\omega=2\pi f$ – the angular frequency, f – the frequency of feeding, Jsz – the current density component along z direction.

The integration of equation 1 yields to the finite elements formulation of projective type below:

(2) $$\iint_\Omega \alpha_i\left(-\frac{\partial}{\partial x}\left(\upsilon\frac{\partial A_z}{\partial x}\right)-\frac{\partial}{\partial y}\left(\upsilon\frac{\partial A_z}{\partial y}\right)\right)dxdy \; + \; j\omega\iint_\Omega \alpha_i\sigma A_z dxdy - \iint_\Omega \alpha_i J_{sz} dxdy = 0$$

Using the Green theorem and imposing boundary conditions of homogenous Direchlet type on the boundary of the studied domain, equation 2 becomes:

(3) $$\iint \upsilon\overrightarrow{\nabla\alpha_i}\,\overrightarrow{\nabla A_z}dxdy + j\omega\sigma\iint \alpha_i Azdxdy - \iint J_{sz}\alpha_i dxdy = 0$$

(4) $$A_z = \sum_{j=1}^{n}\alpha_j A_j$$

where: υ =1/μ, α_i – screening function, α_j – shape function associated with the node j.

Discrete shape functions are employed to recast the problem as a set of simultaneous algebraic equations, given by [9]:

(5) $$([M]+j\omega[L])[A]=[K]$$

where: *[M]* – stiffness matrix, *[L]* – dynamic matrix, *[K]* – source vector, *[A]* – vector of the unknown.

Impedance computation

The coil impedance computation with and without the crack may be obtained using a general method based on the evaluation of the magnetic flux as indicated in equation 6 and 7. [10]

(6) $$\mathrm{Re}(Z) = -\frac{N^2}{JS^2}\omega\iint_s 2\pi r\,\mathrm{Im}(A)ds$$

(7) $$\mathrm{Im}(Z) = -\frac{N^2}{JS^2}\omega\iint_s 2\pi r\,\mathrm{Re}(A)ds$$

where: *Re (Z) and Im (Z)* – the real and imaginary parts of the impedance of the coil respectively, *N and S* – the number of turns coil and the surface of the conductor respectively.

Inverse problem resolution with neural networks

Artificial neural networks are non-linear data driven self-adaptive approach. They are powerful tool for modeling, especially when the underlying data relationship is unknown. They are known for a few years with increasing success in various fields and they are widely used in nondestructive testing using eddy currents. The use of non-conventional approaches for NDT, such as neural networks, is justified by the difficulty of finding a proper solution to this problem by using standard methods. The most widely used neural classifier is the Multi-Layer Perceptron (MLP) [7, 11].

For this work, the objective of this technique is the use of the impedance of the probe as input to neural network to identify and evaluate the shape of the crack towards the outlet of neural network. As regards the choice of the neural network model (network structure and the setting of internal parameters), which is an important step in the inversion process; a multilayer perceptron MLP was used for its intrinsic ability to perform highly complex tasks in a very short time. This choice was also supported by most of the literature.

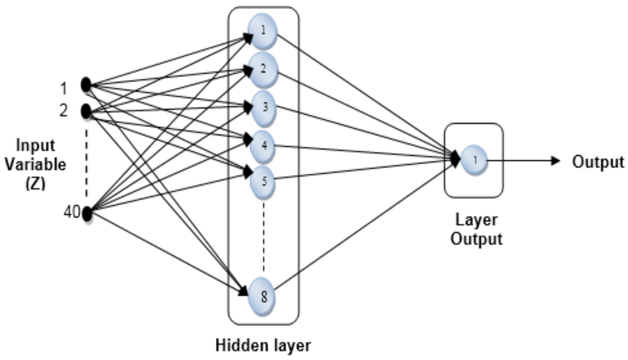

Fig. 2. Used network architecture

The neurons of each layer are connected with all the neurons of the previous layer. Nodes comprise the weighted sum of the nodes in the earlier layer passed through a transfer function, for example, the sigmoid function. The connection weights are the free parameters of a learning process. They are determined by presenting to the network a set of actual input-output values (the training set). During the learning process the network output and the desired output are compared through the error function called mean square error (MSE), calculated by [7, 12].

(8) $$MSE(w)=\frac{1}{N}\sum_{k=1}^{N}\left\|D_k-S\left(E_k,w\right)\right\|^2$$

where: *[E_k]* – input vector, *[D_k]* – desired output vector, *[w]* – constituted column vector of the set of the weights and bias of the network, *S* – the realised function by NN, *N* – number of samples in the training set.

Introduced network is a multi-layers perceptron called ”Feed-forward”, it is a static network having two layers, a layer hidden from 8 neurons with a function of tangent sigmoid activation and an output layer in the single neuron with a function of linear activation Fig. 2. As in the most part of applications presented in literature, the size of hidden layer has to be heuristically determined. [13].

For its training we used the algorithm of Levenberg-Marquardt which is an approximation of Newton’s method. If a function V(x) is to be minimized with respect to the parameter vector x, then Newton’s method would be [12]:

(9) $$\Delta \underline{x}=-\left[\nabla^2 V\left(\underline{x}\right)\right]^{-1}\nabla V\left(\underline{x}\right)$$

where: $\nabla^2 V\left(\underline{x}\right)$ – hessian matrix, $\nabla V\left(\underline{x}\right)$ – gradient.

Experimental set-up

The experimental system shown in Fig. 3 consists of an impedance analyzer, an EC sensor and a plate without defect. All other elements, the generator, the amplifier, the demodulator and the display, are mounted in a compact manner inside the AGILENT 4294A.

For the eddy current sensor, it is a single coil (double function), the measurement is absolute. The measured signal is the impedance of the coil which plays both the role of transmitter and receiver.

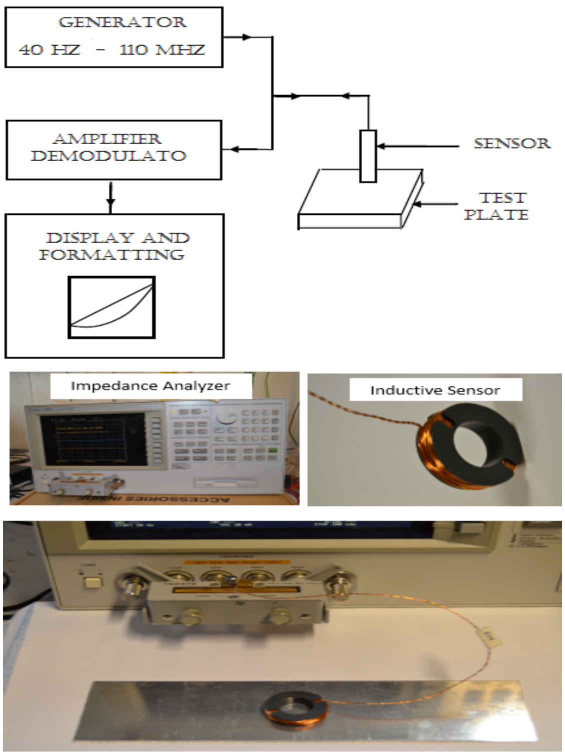

Fig. 3. Measuring system

The impedance data of the coil were recorded using an impedance analyzer type "Agilent 4294A" . The impedance analyzer is a fairly accurate device that allows us to scan a wide range of frequencies ranging from 40 Hz to 110 MHz. It makes it possible to visualize and measure the modulus of the impedance |Z| (f1, f2,...) and the phase θ (f1, f2,...) of the coil / piece system in a determined frequency range.

The analysis is carried out for a fixed position of the plate with different frequencies (f=1,4kHz - 1,6kHz). The impedance values have been acquired for each value of the frequency.

Results and discussion

Validation of the faultless EF code

After solving the magnetodynamic partial differential equation using finite element program developed under Matlab package, as well as some experimental tests, the results obtained for the two kinds of materials are given in figure 4, in terms of impedance variation versus respect different values of the frequency (1.4 kHz-1.6 kHz).

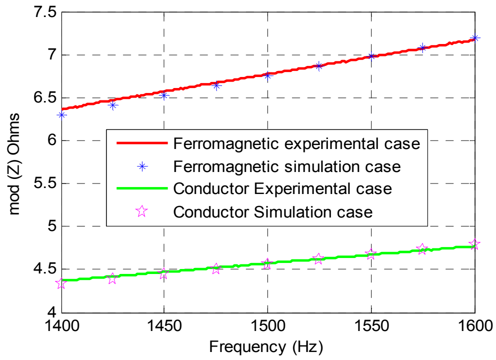

Fig. 4. The impedance variation as function of frequency

In figure 5, the results representing the variation in relative value impedance of a ferromagnetic and non-ferromagnetic material are presented.

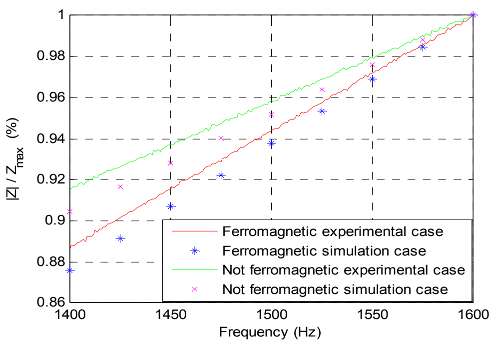

Fig. 5. The impedance variation as function of frequency in relative value

Figure 6 gives the variation of the phase of the signal with respect to the frequency, which is measured in the impedance plane

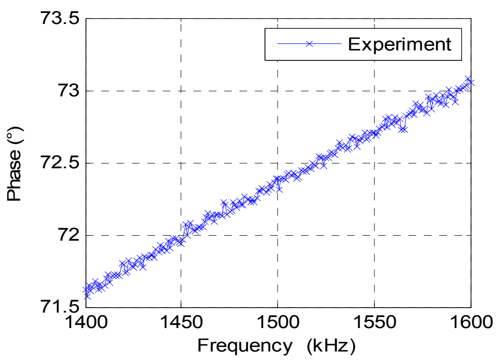

Fig. 6. The phase variation as function of frequency

We observe that for each operating frequency corresponds a value of |Z|/Zmax and it is from there that we can make the difference between the two materials. For exemple, f=1400 Hz, it can be seen that for a ferromagnetic, |Z|/Zmax represents an average of 87% of its value, and for a conductor an average of 91%.

Surface defects detection

The simulation results obtained in case of single defect figure 1 (c) when considering a relative magnetic permeability of the plate μ_r= 1,2 and a value of electrical conductivity of 1 Ms/m, are given in terms of impedance variation (difference impedance) versus sensor position for different values of frequency (1,4 kHz, 1,5 kHz and 1,6 kHz) figure 7, and for different values of the lift-off figure 8.

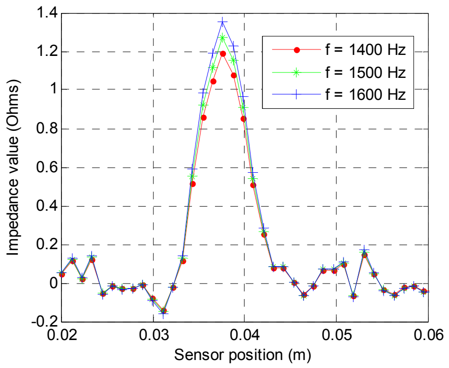

Fig. 7. The impedance variation as a function of sensor position for different values of frequency

The variation of the impedance as a function of sensor position reflects the variation of the distribution of properties in a test sample in the presence of defects.

The impedance changes depending on the position of the sensor for different values of lift-off for a sensor power supply frequency of 1.5 kHz.

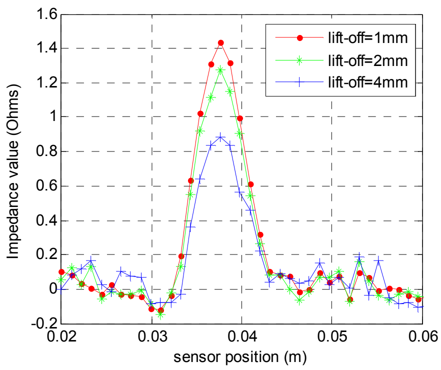

Fig. 8. The impedance variation as function of sensor position for different values of lift-off

The lift-off describes the distance between the sensor and the plate. By varying the lift-off the magnetic coupling between the sensor and the plate decreases, and the influence of the plate on the sensor becomes less important.

Figure 9 gives the variation of the impedance for the electrical conductivity values ranging from 1 to 4 Ms/m.

When the conductivity of the plate is increased, the crack currents become larger.

Figure 10 gives the variation of the impedance for different values of relative magnetic permeability (1,2 to 100) with a frequency of 1,5 kHz and an electrical conductivity of plate of 1 Ms/m.

When the relative magnetic permeability of the plate is varied, it is perceived that the μ_r disturbs the measurements and affects the correct detection of the defect. Figure 11 shows the results obtained in case of multiple defect

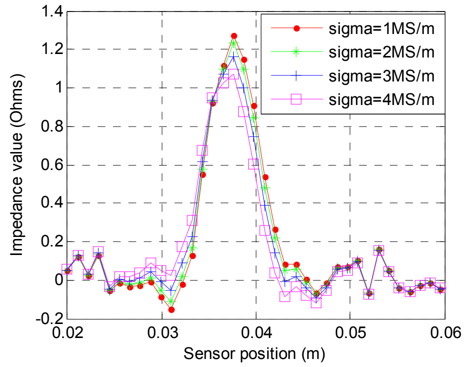

Fig. 9. The impedance variation as a function of sensor position for different values of electrical conductivity

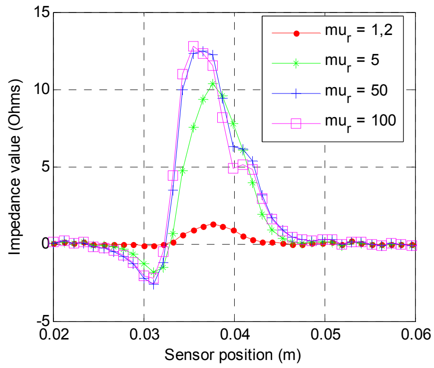

Fig. 10. The impedance variation as function of sensor position for different value of relative magnetic permeability

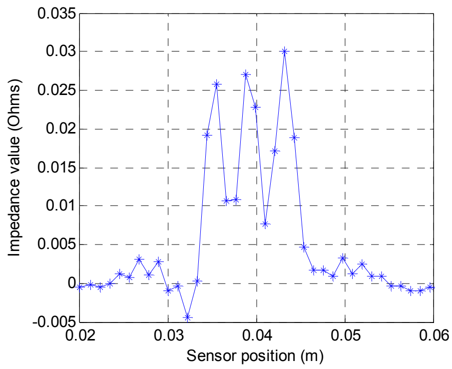

Fig.11.The impedance variation as function of sensor position in case of multiple defects [Fig.1.d]

Caracterisation of surface cracks

Methodologies to be adopted for defect feature identification by means of neural network on the basis of NDT are given below:

1) Prepare data set for neural network from non-destructive tests.

2) Develop neural network using MATLAB (choose a structure , number of inputs, number of outputs and number of layers and select transfer functions and a learning algorithm).

3) Validation of results with respect to actual greatness.

The impedance of the eddy current probe is introduced as input to the neural network and the shape of the defect and its dimensions are measured by the output of the network figure 12.

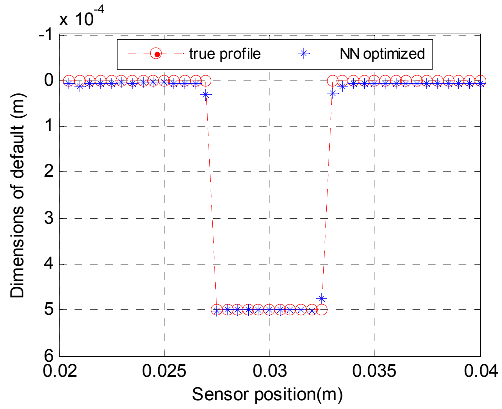

Fig.12. Reconstruction of the depth and height of defect (single defects)

For this case, the resolution time is 8 seconds, the stopping criteria consists of a maximum number equals to 1000 epochs, a minimum error gradient equal to 10E-12, and a minimum mean square error equals to 10E-10.

To test the robustness of the network, we have tried to reconstruct a series of defects, and the output of the neural network is given in figure 13.

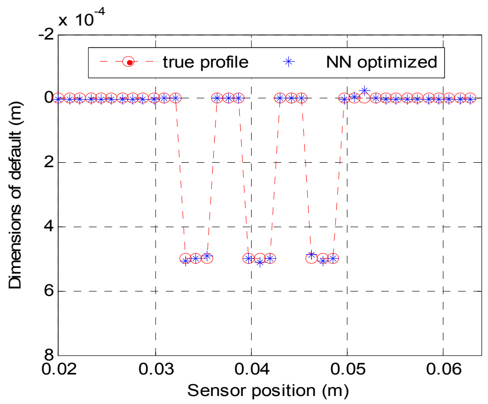

Fig.13. Reconstruction of the depth and height of complex defect (multiple defects).

For this case, the resolution time is 10 seconds, the stopping criteria consists of a maximum number equals to 1000 epochs, a minimum error gradient equal to 10E-12, and a minimum mean square error equals to 10E-11. CPU running frequency is 2,16 GHz with 2 Go RAM, and precision of data it's 32 bits.

Conclusion

This work introduces the use of the neural networks technique for the reconstitution of defects in a ferromagnetic plate. This inversion technique has been validated for the reconstitution of a single and multiple defects occurring in the material.

The database is constructed from the resolution by finite element method of direct problem in terms of impedance variation of the sensor and is introduced as input values of the neural networks algorithm build under Matlab environment. The depth and the height of defects reconstitution is realized successfully and with much reduced time computation. After comparison with the real dimensions, the results seem to be in good agreement.

For validation purpose of the finite element code (FE), comparisons of simulation and experimental are performed in first part for a non ferromagnetic and a ferromagnetic material, where a good agreement could be note.

***Authors**: PhD student. Hamid Mehaddene, Department of Electrotechnics, Mouloud Mammeri University of Tizi-Ouzou, BP 17RP 15000, Algeria, E-mail: mehaddenehamid@yahoo.com; prof. dr. Hassane Mohellebi, Department of Electrotechnics, Mouloud Mammeri University of Tizi-Ouzou, BP 17RP 15000, ALGERIA, E-mail: mohellebi@yahoo.fr; PhD student. Azouaou Berkache, Department of Electrotechnics, Mouloud Mammeri University of Tizi-Ouzou, BP 17RP 15000, Algeria, E-mail:azouaoubrk@yahoo.fr*

REFERENCES

[1] Grimberg R., Electromagnetic Nondestructive Evaluation: Present and Future, *SV-JME*, 57(2011), No. 3, 204–217.
[2] Janousek L., Capova K., Yusa N., Miya K., Multiprobe Inspection for Enhancing Sizing Ability in Eddy Current Nondestructive Testing, *IEEE Trans. Magn*., 44 (2008), No. 6, 1618-1621.
[3] Hamel A., Mohellebi H., Féliachi M., Imperialist Competitive Algorithm and Particle Swarm Optimization Comparison for Eddy Current Non-destructive Evaluation, PRZEGLĄD ELEKTROTECHNICZNY (Electrical Review), R. 88 NR 9a/2012, ISSN 0033-2097.
[4] Marco R., Giuseppe S., Luigi F., Marco L., Ibukun D-A., Gui Y-T., Evaluation of the Lift-off Robustness of Eddy Current Imaging Techniques, *NDT & E International.*, http://dx.doi.org/10.1016/j.ndteint.2016.10.001
[5] García-Martín J., Gómez-Gil J., Vázquez-Sánchez E., Nondestructive Techniques Based on Eddy Current Testing, *Sensors*, 11 (2011), 2525-2565
[6] Lorenzi A., Silva Filho L-C-P-da., Artificial Neural Networks Methods to Analysis of Ultrasonic Testing in Concrete, *the e-Journal of Nondestructive Testing.* 20 (2015), No. 11, ISSN 1435-4934
[7] Ayad A., Benhamida F., Bendaoud A., Le Bihan Y., Bensetti M., Solution of Inverse Problems in Electromagnetic NDT Using Neural Networks, *PRZEGLĄD ELEKTROTECHNICZNY* (Electrical Review), R. 87 NR 9a(2011), ISSN 0033-2097
[8] Haoyu H., Toshiyuki T., Tetsuya U., Fast Numerical Calculation for Crack Modeling in Eddy Current Testing of ferromagnetic materials, *Journal of Applied Physics,* 94(2003)., No. 9, 5866-5872
[9] Mingye Y., Satish U., Shreekanth M., Yushi S., Paul S., William L., Solution of Inverse Problems in Electromagnetic NDE Using Finite Element Methods, *IEEE Transactions on Magnetics*, 34(1998)., No. *5*, 2924-2927
[10] Thomas J-L., Modeling Simplified by Control by Eddy Current of Type of Generator of Steam report of internship ESA IGELEC, 1998, University of Nantes, France
[11] Francesca C., Alessandra F., Augusto M., Pietro T., Mariangela U., Artificial Neural Networks for Non-Destructive Evaluation with Ultrasonic Waves in not Accessible Pipes, *IEEE,* 6(2005), No. 05, 685-692
[12] Martin T., Hagan., Mohammad B., Menhaj., Training Feedforward Networks with the Marquardt Algorithm, *IEEE, Trans, Neural Networks*, 5(1994), No. 6, 989-993
[13] Lande P-S., Gadewar A-S., October 2012. Application of Artificial Neural Networks in Prediction of Compressive Strength of Concrete by Using Ultrasonic Pulse Velocities, IOSR Journal of Mechanical and Civil Engineering (IOSR-JMCE), 1 (2012) No. 3 ISSN: 2278-1684, PP 34-42